

Effect of heat treatment on the crystallization toughening of tailing-derived glass-ceramics

Du Yongsheng^a, Yang Xiaowei^a, Zhang Hongxia^a, Zhang Xuefeng^a, Zhao Ming^b, Chen Hua^a, Ouyang Shunli^b and Li Baowei^{b,*}

^aCollege of Science, Inner Mongolia University of Science & Technology, Baotou 014010, China

^bKey Laboratory of Integrated Exploitation of Bayan Obo Multi-Metallic Resources, Inner Mongolia University of Science and Technology, Baotou 014010, China

The effect of heat treatment to a parent glass of the composition CaO-MgO-Al₂O₃-SiO₂ (CMAS) on the course of crystallization and properties of the Bayan Obo east mine tailing glass-ceramics is examined. The crystallization behavior, phase composition, morphology and structure of glass-ceramics are characterized. The results indicate that the phases formed in the glass-ceramics are augite and the initial nucleation phases are magnetite, which can be proved by differential scanning calorimetry (DSC), X-ray diffraction (XRD) and scanning transmission electron microscope (STEM). Heat treatment plays a significant role in improving the crystallization process, fracture characteristics, modulus and bending strength. All of these properties reach a maximum for the fully crystallized glass-ceramic. Scanning electron microscope (SEM) and atomic force microscope (AFM) are used to reveal the topography of the fracture surfaces. The intergranular fracture can be observed on the fracture surface.

Key words: Bayan Obo east mine tailing, Glass-ceramics, Heat treatment, Fracture surfaces, Fracture toughness.

Introduction

The rapid industrial development based on extremely high resource consumption has resulted in huge amount of emissions and accumulation of various tailings, slag and fly ash, which have brought great harm to environment. At present, the method of treatment and comprehensive utilization of large amount of above-mentioned solid wastes include landfill, stockpile, paving, cement production, etc. However, these treatment methods in part exist some limitations and deficiencies, such as high cost, high energy consumptions, low value-added products and easy to create secondary contamination. The productions of glass-ceramics using solid waste as the raw materials have opened up a new way for the cleaning, high value and efficient utilization of solid wastes, which demonstrate the possibilities of recycling solid waste to resolve environmental and ecological problem [1-3]. Especially, glass-ceramics with augite as main crystalline phases attract interest in several advanced fields as they offer excellent mechanical properties which can be used as abrasion-resistant or high chemical durability materials [4]. In our earlier work, Bayan Obo mine tailing glass-ceramics based on augite have shown outstanding strength, excellent abrasion and chemical resistance and

it can be recognized as potential candidates for various structural applications [5-8], such as building materials, machinable ceramics or machinery mining, etc. Glass-ceramics are polycrystalline materials and produced by the controlled crystallization of glasses. The crystallization behavior is an important effect that determines the properties, which can be determined by heat-treatment, chemical composition, or the employed nucleating agents. J.F. Wu reported the crystallization behavior and properties of K₂O-CaO-Al₂O₃-SiO₂ glass-ceramics [9]. It can be found that the crystalline phases and microstructures of the glass-ceramics are obviously affected by the sintering process. Gao Qu has reported that heat treatment has an effect on volume fraction of the crystalline phases and the microstructure of the glass-ceramics [10]. In addition, a change in heat-treatment temperature will cause a significant change in the mechanical properties. Concerning the crystallization process for tailing glass-ceramics, several references indicated that glass composition, crystalline phase and structure characteristics will influence the performance of the final materials [11-13].

However, glass-ceramic is considered to be typical hard-to-machine material for its high hardness, high brittleness and low fracture toughness. The low fracture toughness directly limits the application of glass-ceramic as a structural material. Controlled crystallization of glass-ceramic can be regard as an effective toughening method which can be carried out by heat-treatment. The hardness, elastic modulus, flexural strength and fracture toughness reached a maximum for the fully crystallized

*Corresponding author:
Tel : +86-472-5954358
Fax: +86-472-5954358
E-mail: 46588582@qq.com

glass-ceramic. In this work, in order to investigate deeply the effect of crystallization behavior of Bayan Obo east mine tailing glass-ceramics on the properties, the tailing glass-ceramics with different heat treatment were prepared and the fracture behavior, hardness, Young's modulus and fracture toughness are discussed in detail.

Experimental Procedure

The experimental tailing and fly ash were obtained from Baotou Iron and Steel Company of China and Huadian Generating-Electricity Co., Ltd, respectively. The major chemical compositions of Bayan Obo east mine tailing and fly ash were shown in our previous study [14]. Bayan Obo east mine tailing contributed mainly to CaO and TFe (total Fe) compositions while fly ash to SiO₂ and Al₂O₃. The basic composition of the parent glass, 42.60% SiO₂, 27.20% CaO, 3% MgO and 5.50% Al₂O₃ (all the compositions are referred to wt%) was selected. 42.3 wt% of tailing and 17 wt% of fly ash were used as raw materials to prepare CaO-MgO-Al₂O₃-SiO₂ (CMAS) glass ceramics and SiO₂, Al₂O₃, MgO, and CaO (chemical grade) were used to compensate the compositions which cannot be matched by the tailing and fly ash. No additional nucleant agents were added for the crystallization of the glass since the content of total Fe in glass-ceramics were about 9.2 wt% which derived from raw materials.

The process of making glass-ceramics included glass melting, annealing, nucleation and crystallization stage, and so forth. Firstly, the Bayan Obo east mine tailing, fly ash and other additives were mixed together after grinding. The well-mixed batches were melted in an electric furnace at 1450 °C for 3 hrs using corundum crucible to form homogeneous melts, then the melts were cast into preheated stainless steel moulds and subsequent annealing at 600 °C for 2 hrs. The annealed glass samples were placed in a muffle furnace for the nucleation and crystallization treatments, while the nucleation temperature and crystallization temperature (T_p) were determined by differential scanning calorimetry (DSC) measurement. After the crystallization treatment, the samples were furnace cooled to room temperature before the property examinations.

Thermo behaviors of the parent glasses directly cast in water were examined by a DSC measurement (Netzsch DSC 404 F3), applying temperature accelerating rate of 10 °C/min. The phase constituents of the glass-ceramics were identified by X-ray powder diffraction (XRD, Bruker diffractometer, AXS D8 Advanced). The microscopic structures were investigated by scanning electron microscope (SEM, Philips, Quanta 400). The scanning transmission electron microscope (STEM) was performed on a Tecnai G2 F20 STwin electron microscope operated at 200 kV acceleration voltage. Three dimensional surface morphology of the sample

were analyzed using an atomic force microscope (AFM, MFP-3D-SA, Asylum Research). Before conducting AFM, the surfaces were cleaned with ethanol to remove dust and other contaminants and dried with compressed air. Elastic constants of the glass-ceramics, including Young's modulus (E), shear modulus(G) and Poisson's ratio(ν), were measured using resonant ultrasound spectroscopy (RUS) [15]. The three-point bending strength of rectified parallelepiped bars (3 mm × 4 mm × 40 mm) of glass-ceramics was tested by the CSS-88000 electronic universal testing machine. Each value is the mean value of measurements made with five samples. Indentation experiments were conducted using a Vickers hardness tester (HV-SOA). A load of 3 N and a dwell time of 10 s were used to make indents on the polished surface of samples. Six indentation experiments were measured and the average value was calculated. Vickers impression morphology of glass-ceramics was observed by laser confocal microscope (LEXT OLS4000). The densities were measured by Archimedes method. The corrosion test was measured according to the cast stone standard JC/T258-1993 with a concentration of 20% H₂SO₄, and diameter of 0.5 mm-1.0 mm glass-ceramic pellets for water bath heating of 100 °C.

Results and Discussion

Fig. 1 shows the DSC plot of parent glass. Apparent transition temperature (T_g) at 635 °C is observed, followed by two crystallizing exothermic peak at 745 and 825 °C, respectively. It can be deduced that the small exothermic peak is associated with the temperature that yields a high nuclear density throughout the interior of the glass and the large exothermic peak (T_p) is associated with the production of nuclear growth at a reasonable rate. The two exothermic crystallization peaks could be associated to the formation of magnetite nuclei and augite, respectively. Thus, a conventional two stage-heat treatment can be performed and the nucleation and crystallization temperatures are selected as 720 °C and 850 °C, respectively. Both of the above two heat

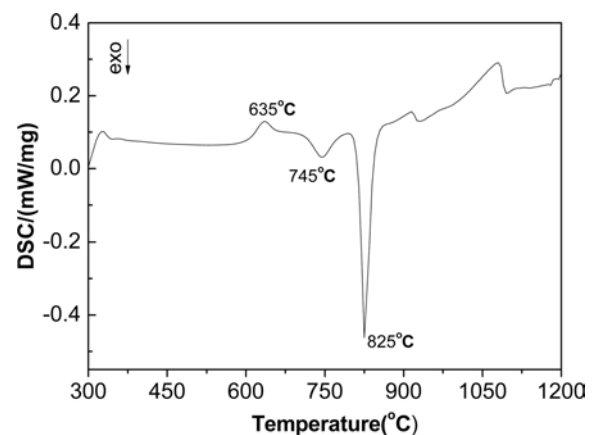


Fig. 1. DSC curve of the parent glass.

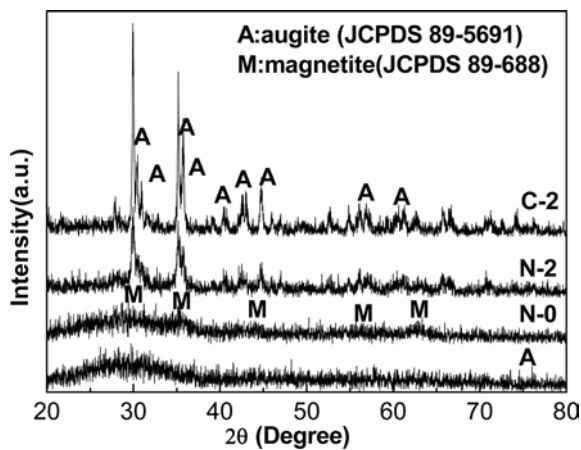


Fig. 2. XRD spectra of sample with different heat treatment.

treatment time is 2 hrs.

Fig. 2 presents the XRD patterns of the glass samples subjected to sequential heat treatments. Where Sample A is the annealed one without nucleation process, Samples N-0 and N-2 are treated by a nucleation process and the nucleation time is zero (heated to 720 °C and directly cast in water) and 2 hrs, respectively. Sample C-2 is carried out by nucleation and crystallization process. The appearance of a broad halo and the absence of any diffraction peaks associated with crystalline phases in Sample A indicate that the annealed sample has only glassy structure. The weak peaks of magnetite (Fe_3O_4 , JCPDS 89-688) with cubic spinel structure appear in the initial stages of nucleation. After the nucleation treatment for 2hrs, the sample's crystallinity change obviously and the intensity is relatively higher. It can be found that the peaks of augite ($\text{Ca}(\text{Mg},\text{Fe},\text{Al})_2(\text{Si},\text{Al})_2\text{O}_6$, JCPDS 89-5691) appear in the crystallization treatment for 2hrs, which suggest that these magnetite might induce the crystallization of residual glass matrix, resulting in the crystallization of augite [16].

In order to research the effect of crystallization behavior on the molecule structure and vibrational of chemical bond of glass-ceramics, the samples with different heat treatment are detected by Raman spectra and the results are shown in Fig. 3. It is well known that the different wave number of Raman spectra can reflect the structural characteristics of glass-ceramic. That is, the low wave number ($< 400 \text{ cm}^{-1}$) correspond to the long-range ordered silicate structure, which reflect the vibration between metal and oxygen and only appear in the crystal. In our measurements, it can be found that both the intensity and numbers of peak of Raman spectra also increase with the increase of heat treatment temperature. The above phenomena show that the degree of crystallization of glass-ceramics is gradually increased, which corresponds to the result of XRD. The wavenumbers range of $400\text{--}800 \text{ cm}^{-1}$ of Raman spectra is related to stretching or bending vibrations of bridge oxygen within silicon-oxygen $[\text{SiO}_4]^{4-}$ tetrahedrons.

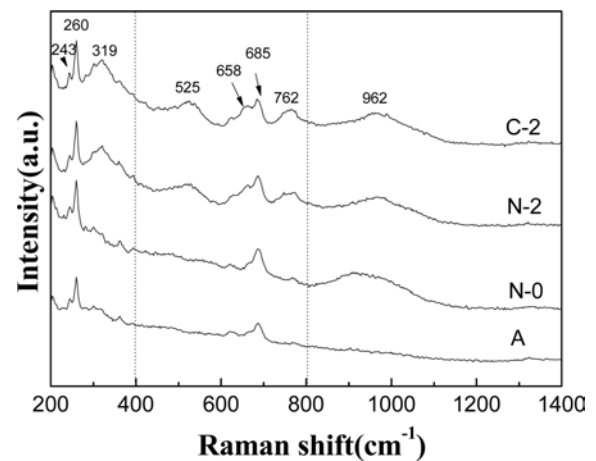


Fig. 3. Raman spectra of glass-ceramic with different heat treatment.

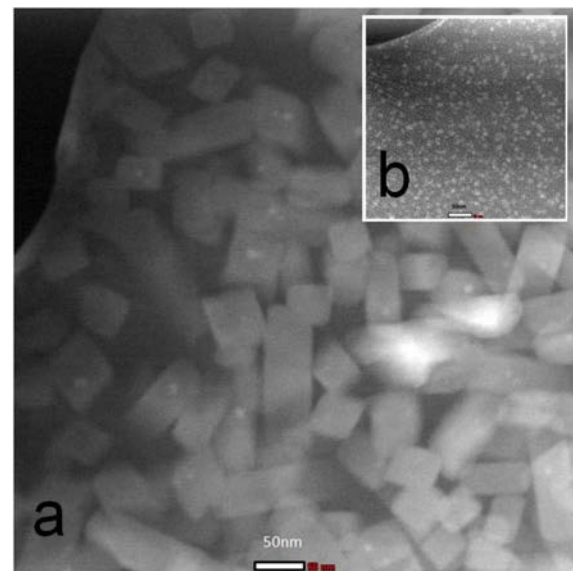


Fig. 4. STEM micrograph of sample C-2 (a) and sample N-0 (b).

The band at 525 cm^{-1} is mostly associated with stretching vibrations of fully polymerized silicon-oxygen tetrahedrons. The band at 658 cm^{-1} is related to the symmetric bending vibrations of Si-O-Si and the band at 685 cm^{-1} is characteristic for symmetric stretching vibrations of Si-O-Si. The increase in Raman bands indicate that heat treatment schedule increase the silicate sub-network polymerization level.

STEM of some selected samples are shown in Fig. 4. The crystallization of one or different phases is evidenced in STEM micrographs. STEM reveal precipitation of nano size short columnar crystals of augite phase dispersed in amorphous glassy phase in the sample C-2 and a large proportion of the crystalline phase show a high degree of crystallinity. Sample N-0 is also analyzed by STEM and it can be found that droplets sized 5-10 nm is distributed homogeneously among the glass matrix. The white droplets in sample C-2 correspond to Fe-rich phase as the Z number of Fe

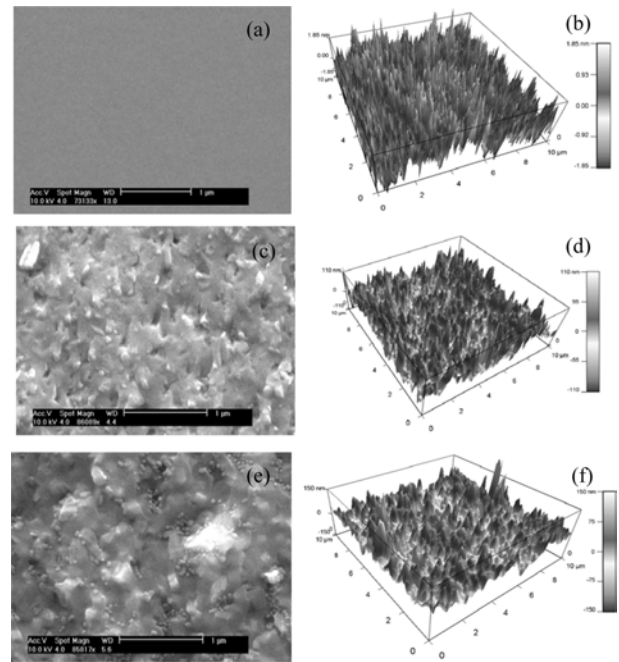
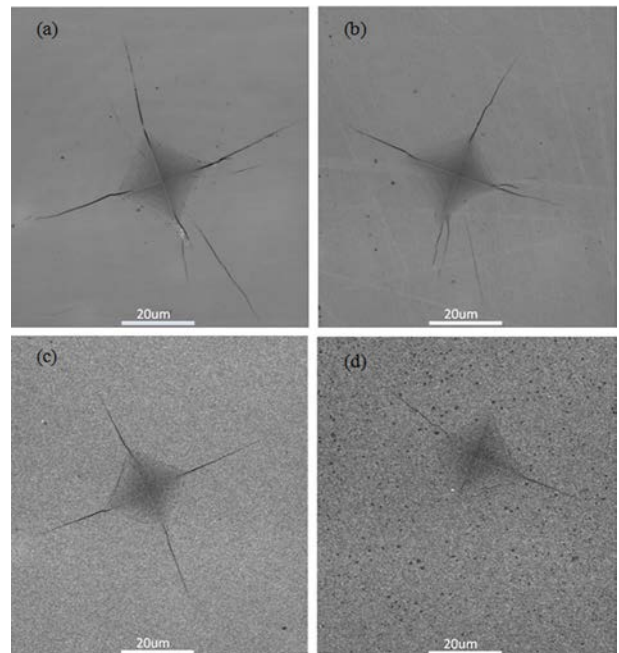
Table 1. The properties of glass-ceramics with different heat treatment.

Sample no.	Density (g/cm ³)	Bending strengths (MPa)	Acid-resistance (%)
N-0	2.67	84.7	47.5
N-2	2.93	125.3	66.4
C-2	3.19	185.9	92.7

is the highest compared with Ca, Mg, Si, Al, and so forth in glass-ceramics since the dark field STEM image can provide an observation of a composition image which means that the bright regions contain a larger amount of elements with higher atomic number. The interfaces of the two phases of Fe-rich phase and Si-rich phase provide the core of heterogeneous nucleation for the consequent precipitation of augite crystalline [17].

In order to evaluate the effect of different heat treatment on the physical and mechanical properties of the glass-ceramics, the density, bending strength and acid-resistance of all samples are measured accordingly and the results are summarized in Table 1. It can be found that the least value of bending strengths is 84.7 MPa and the most value is 185.9 MPa. The difference in bending strength may be attributed to the different degree of crystallinity of glass-ceramics [18]. It is well known that the crystallite phase is increased with the process of heat treatment, which can improve the mechanical property of glass-ceramic. The sample C-2 has the fine crystallite compared with other samples, which can be proved by the XRD results, and this result is likely attributed to increasing the value of bending strengths. Where, the difference in density may also be attributed to the degree of crystallization. Generally, more fine grain size and higher degree of crystallization can improve the density. Uniform crystallization seemingly occurs over the entire bulk of glass-ceramics when the glass is carried out by nucleation and crystallization process. The results of acid-resistance of the present glass-ceramics after leaching in acid solutions are shown that the sample C-2 has higher chemical durability to acid compared with other samples. The highest acid-resistance of sample is derived from the high degree of crystalline which can be proved by density results, since the solubility of the residual glass in acid solution is higher than that of crystalline phase.

Since the fracture properties of glass ceramics have a close relationship with the bending strength, intensive study of fractured surfaces of glass-ceramics can reveal more about the factors affecting the bending strength [19]. Fig. 5 shows the SEM and AFM images of fractured surfaces of the glass-ceramics treated by different heat treatment processes after measuring the bending strength. It can be seen that the sample N-0 has a flat section and no crystals can be detected in fractured surfaces, which is consistent with the results

**Fig. 5.** SEM images (a,c,e) and AFM images (b,d,f) of fractured surfaces of the glass-ceramic with different heat treatment: (a,b) N-0; (c,d) N-2; (e,f) C-2.**Fig. 6.** Vickers impression morphology of glass-ceramics with different heat treatment: (a)A;(b) N-0;(c) N-2;(d) C-2.

of XRD and STEM since the weak initial nucleation phase is very difficult to observe. Small amounts of nanocrystal of augite exist in sample N-2 and the fractured surface is rough compared with sample N-0. Short columnar crystals can be found in sample C-2 and the surface roughness further increase. Meanwhile, a small amount of nano spherical crystal can also be found which correspond to the magnetite crystal

Table 2. The modulus and fracture toughness of glass-ceramics with different heat treatment.

Sample no.	Young's modulus (Gpa)	Shear modulus (Gpa)	Poisson's ratio	Vickers hardness (Gpa)	Fracture toughness (Mpa*m ^{1/2})
N-0	83.65	35.57	0.287	5.74	1.16
N-2	94.15	37.54	0.254	6.48	1.23
C-2	103.96	42.83	0.214	8.11	1.56

nucleus. It can be estimated from Fig. 4 that the fracture mode in the glass-ceramics exhibits a typical brittle fracture pattern and the grains are pulled out on the fracture surface. Furthermore, the glass phases in glass-ceramics also leave a trail of destruction in grain boundary. The result indicate that fracture occurs mainly in a intergranular fracture fashion with pull-out of the grains since the fracture occurs mainly in the location of the intersection of the grain and glass [20-21].

Fig. 6 shows the images of the Vickers indents made at load $P = 3$ N. As it is seen, the indentation diagonals and lengths of the radial cracks have a decreasing tendency with the increase of the heat treatment temperature. Furthermore, it can be found that the cracks change their propagation direction. In samples A and N-0, cracks are visible not only along the median line of the indent, but appear in the adjacent positions in random order. Since there are large numbers of micro cracks in the samples without crystallization, cracks begin to expand from the micro cracks and form different lengths of cracks under external force. As the degree of crystallization increases, the existence of crystal phase significantly suppressed the crack growth. As a result, cracks can mainly propagate along the median line of the indent.

Table 2 shows the effect of different heat treatment on the elastic properties, hardness and fracture toughness of glass-ceramics. In general, the Young's modulus (E), shear modulus (G) and Poisson's ratio (ν) are considered to be important for the characterization of elastic properties of materials. Usually, the polycrystalline elastic properties have higher practical application value than the single-crystal elastic properties. It can be found the shear modulus and Young's modulus increase linearly with the increase in degree of crystallinity. The Young's modulus is 83.65 GPa for the glass and 103.96 GPa for the fully crystallized glass-ceramic and our values agree with those in Ref. [22]. Sample C-2 has the maximum value of Young's modulus and shear modulus, while it has the minimum value of Poisson's ratio. The above phenomenon is directly related to the degree of crystallization of glass-ceramics. Large atomic rearrangements occur at the transformation stage with the process of heat treatment. In such a transformation stage, atomic arrangements might be considerably orderly, giving increase in shear modulus and Young's modulus. It is well known that the Poisson's ratio

of oxide crystalline materials is usually 0.2-0.3. The glasses can be divided into resilient glasses ($0.15 < \nu < 0.20$), semi-resilient glasses ($0.20 < \nu < 0.25$), easily damaged glasses ($0.25 < \nu < 0.33$) [23]. For glass-ceramics, poisson's ratio show a trend to lower values with increasing number of bridging-oxygen per tetrahedron [24]. The improvement of crystallinity can help increase bridging-oxygen in glass-ceramics, which decrease the value of Poisson's ratio. In addition, the hardness of glass-ceramics also show a gradual increase trend with the increase in degree of crystallinity. The large increase of hardness value may be interpreted by the formation of augite. As augite content increases, the structures are more compact with fine packing and hence its hardness values increase.

As a quantitative index for measuring the toughness of material, fracture toughness can be used to characterize the ability for determining the resistance of crack propagation. As a typical brittle material, the fracture toughness of the glass-ceramic represents the key parameter that can be used as a structural material. The calculation formula of fracture toughness is shown as follows:

$$K_{IC} = 0.016 \left(\frac{E}{H_V} \right)^{1/2} \left(\frac{P}{c^{3/2}} \right) \quad (1)$$

where E is Young's modulus, H_V is Vickers hardness, P is apply load, c is the length of surface radial cracks. The variation of fracture toughness with different heat treatment is presented in Table 2 and it can be found that the fracture toughness significantly improved, reaching a maximum of 1.56 MPa*m^{1/2}. It is seen that the higher value can be determined by the improvement of the crystallinity. Crack deflection and crack trapping may contribute to the increased fracture toughness of glass-ceramics. The crystal in glass-ceramic can act as an obstacle to prevent crack propagation as the crack advances and encounters a crystal.

Conclusions

The crystallization behavior and properties in CMAS glass-ceramics derived from Bayan Obo east mine tailing have been investigated as a function of heat treatment. The XRD and DSC analysis shows that the heat treatment promotes the precipitation of augite from the glass matrix, while magnetite can act as the core of nucleation for the consequent precipitation of augite crystalline. The sample N-0 has bending strengths of 84.7MPa, acid-resistance of 47.5%, density of 2.67 g/cm³, Young's modulus of 83.65 GPa, shear modulus of 35.57 Gpa and Poisson's ratio of 0.287. The glass-ceramics after heat treatment has bending strengths of 185.9 MPa, acid-resistance of 92.7%, density of 3.19 g/cm³, Young's modulus of 103.96GPa, shear modulus of 42.83 Gpa and Poisson's ratio of 0.214, demonstrating that poor mechanical and elastic properties of the tailing glass-ceramics are improved through sufficient crystallization.

The fracture mode in the glass-ceramics exhibits a typical brittle fracture pattern and intergranular fracture may be the dominant fracture mode. The increase in fracture toughness can be mainly contribute to the increased in degree of crystallization.

Foundation Item: Item Sponsored by National Natural Science Foundation of China (Grant no.11564031), Natural Science Foundation of Inner Mongolia Autonomous Region (Grant no.2014MS0106), Major Project of Chinese National Programs for Fundamental Research and Development (973 Program, Grant no.2012CB722802)

References

1. Z.K. Zhang, L. Zhang and A.M. Li, *Waste Manage.* 38 (2015) 185-193.
2. Z.B. Liu, Y.B. Zong and H. Feng, *Trans. Indian Ceram. Soc.* 74 (2015) 29-34.
3. S.M. Wang, C.X. Zhang and J.D. Chen, *J. Mater. Sci. Technol.* 30 (2014) 1208-1212.
4. T. Toya, Y. Tamura, Y. Kameshima and K. Okada, *Ceram. Int.* 30 (2004) 983-989.
5. B.W. Li, Y.S. Du, X.F. Zhang, X.L. Jia, M. Zhao and H. Chen, *J. Ceram. Process Res.* 15 (2014) 325-330.
6. T. Zhao, B.W. Li, Z.Y. Gao and D.Q. Chang, *Mater. Sci. Eng. B* 170 (2010) 22-25.
7. B.W. Li, L.B. Deng, X.F. Zhang and X.L. Jia, *J. Non-Cryst. Solids* 380 (2013) 103-108.
8. B.W. Li, Y.S. Du, X.F. Zhang, M. Zhao and H. Chen, *Environ. Prog. Sustainable Energy* 34 (2015) 420-426.
9. J.F. Wu, Z. Li, Y.Q. Huang and F. Li, *Ceram. Int.* 39 (2013) 7743-7750.
10. Q. Gao, X.L. Hu, L. Cui and A.X. Lu, *Ceram. Int.* 40 (2014) 4213-4218.
11. F. He, Y. Fang, J.L. Xie and J. Xie, *Mater. Des.* 42 (2012) 198-203.
12. H. Shao, K. Liang, F. Peng, F. Zhou and A. Hu, *Miner. Eng.* 18 (2005) 635-637.
13. Y. Zhao, D.F. Chen, Y.Y. Bi and M.J. Long, *Ceram. Int.* 38 (2012) 2495-2500.
14. B.W. Li, Y.S. Du, X.F. Zhang, X.L. Jia, M. Zhao and H. Chen, *Trans. Indian Ceram. Soc.* 7 (2013) 119-123.
15. D.P. Wang, D.Q. Zhao, D.W. Ding, H.Y. Bai and W.H. Wang, *J. Appl. Phys.* 115 (2014) 123507-1-4.
16. A. Karamanov and M. Pelino, *J. Non-Cryst. Solids* 281 (2001) 139-151.
17. S.M. Wang, F.H. Kuang, Q.Z. Yan, C.C. Ge and L.H. Qi, *J. Alloys Compd.* 509 (2011) 2819-2823.
18. Y. Soon-Do and Y. Yeon-Hum, *J. Ceram. Process Res.* 12 (2011) 361-364.
19. A. Theocharopoulos, X. Chen, R.M. Wilson, R. Hill and M.J. Cattell, *Dent. Mater.* 29 (2013) 1149-1157.
20. X.H. Chen, T.C. Chadwick, R.M. Wilson, R.G. Hill and M.J. Cattell, *Dent. Mater.* 27 (2011) 1153-1161.
21. P. Zhang, X.H. Li, J.F. Yang and S.C. Xu, *J. Non-Cryst. Solids* 402 (2014) 101-105.
22. F.C. Serbena, I. Mathias, C.E. Foerster and E.D. Zanotto, *Acta Mater.* 86 (2015) 216-228.
23. P. Sellappan, T. Rouxel, F. Celarie, E. Becker, P. Houizot and R. Conradt, *Acta Mater.* 61 (2013) 5949-5965.
24. M. Tiegel, R. Hosseinabadi, S. Kuhn, A. Herrmann and C. Rüssel, *Ceram. Int.* 41 (2015) 7267-7275.